European Journal of Mechanics A/Solids 50 (2015) 28–38

Contents lists available at ScienceDirect

European Journal of Mechanics A/Solids

journal homepage: www.elsevier.com/locate/ejmsol

Nonlinear stability analysis of thin FGM annular spherical shells on elastic foundations under external pressure and thermal loads

Vu Thi Thuy Anh, Dao Huy Bich, Nguyen Dinh Duc*

Vietnam National University, Hanoi, 144 Xuan Thuy, Cau Giay, Hanoi, Viet Nam

ARTICLE INFO

Article history:
Received 21 May 2014
Accepted 13 October 2014
Available online 22 October 2014

Keywords:
Nonlinear stability analysis
FGM annular spherical shells
Elastic foundations
Thermo-mechanical loads

ABSTRACT

To increase the thermal resistance of various structural components in high-temperature environments, the present research deals with nonlinear stability analysis of thin annular spherical shells made of functionally graded materials (FGM) on elastic foundations under external pressure and temperature. Material properties are graded in the thickness direction according to a simple power law distribution in terms of the volume fractions of constituents. Classical thin shell theory in terms of the shell deflection and the stress function is used to determine the buckling loads and nonlinear response of the FGM annular spherical shells. Galerkin method is applied to obtain closed – form of load – deflection paths. An analysis is carried out to show the effects of material, geometrical properties, elastic foundations and combination of external pressure and temperature on the nonlinear stability of the annular spherical shells.

1. Introduction

Nowadays, with the development of aesthetics, architectures and designs are becoming diversified and abundant. Thus, it requires study of shape and material of structures to be cared.

A considerable number of published researches in recent years have focused on the thermo-elastic, dynamic and buckling analyses of functionally graded material (FGM). This is mainly due to the increasing use of FGM as the components of structures in the advanced engineering. FGM consisting of metal and ceramic constituents have received remarkable attention in structural applications. Smooth and continuous change in material properties enable FGM to avoid interface problems and unexpected thermal stress concentrations. By high performance heat resistance capacity, FGM is now chosen to use as structural components exposed to severe temperature conditions such as aircraft, aerospace structures, nuclear plants and other engineering applications.

As a result, the problems relating to the thermo-elastic, dynamic and buckling analyses of plates and shells made of FGMs have attracted attention of many researchers, especially the FGM spherical shells. Shahsiah et al. (2006) extended their previous works for isotropic material to analyze linear stability of FGM shallow spherical shells subjected to three types of thermal loading. Ganapathi (2007) studied the problem, which is performed on the point of view of small deflection and the existence of type-bifurcation buckling of thermally loaded spherical shells. The nonlinear axisymmetric dynamic stability of clamped FGM shallow spherical shells has been analyzed by Prakash et al. (2007) using the first order shear deformation theory and finite element method. Bich and Tung (2011) have studied the nonlinear axisymmetric response of functionally graded shallow spherical shells under uniform external pressure including temperature effects. Huang (1964) reported an investigation on unsymmetrical buckling of thin isotropic shallow spherical shells under external pressure. Tillman (1970) investigated the buckling behavior of clamped shallow spherical caps under a uniform pressure load. Uemura (1971) employed a two term approximation of deflection to treat axisymmetrical snap buckling of a clamped imperfect isotropic shallow spherical shell subjected to uniform external pressure. Nonlinear static and dynamic responses of spherical shells with simply supported and clamped immovable edge have been analyzed by Nath and Alwar (1978) by making use of Chebyshev's series expansion. Nonlinear free vibration response, static response under uniformly distributed load, and the maximum transient response under uniformly distributed step load of orthotropic thin spherical caps on elastic foundation have been obtained by Dumir (1985). Buckling and postbuckling behaviors of laminated spherical caps subjected to uniform external pressure also have been analyzed by Xu (1991) and Muc (1992). Duc et al. (2014) investigated nonlinear axisymmetric response of FGM shallow spherical shells on elastic foundations.

* Corresponding author. Tel.: +84 4 3754 79 78; fax: +84 4 3754 77 24.
E-mail address: ducnd@vnu.edu.vn (N.D. Duc).

http://dx.doi.org/10.1016/j.euromechsol.2014.10.004
0997-7538/

The annular spherical shell is one of the special shapes of the spherical shells. Despite the evident importance in practical applications, it is a fact from the open literature that investigations on the thermo-elastic, dynamic and buckling analyses of FGM annular spherical shell are comparatively scarce. There has been recently a few of publications on the annular shells. The most difficult in annular shell problems is complex calculations.

Alwar and Narasimhan (1992) investigated the axisymmetric nonlinear analysis of laminated orthotropic annular spherical shells, the object of this investigation is to give analytical solutions of large axisymmetric deformation of laminated orthotropic spherical shells including asymmetric laminates. Wu and Tsai (2004) studied the asymptotic DQ solutions of functionally graded annular spherical shells by combining the method of differential quadrature (DQ) with the asymptotic expansion approach. Dumir et al. (2005) analyzed axisymmetric dynamic buckling analysis of laminated moderately thick shallow annular spherical cap under central ring load and uniformly distributed transverse load, applied statically or dynamically as a step function load. Kiani and Eslami (2013) studied an exact solution for thermal buckling of annular FGM plates on an elastic medium, Bagri and Eslami (2008) generalized coupled thermo-elasticity of functionally graded annular disk considering the Lord–Shulman theory.

To the best of our knowledge, there has been recently no publication on solution of the nonlinear stability analysis (buckling and post-buckling) of thin FGM annular spherical shells on elastic foundations under temperature.

In this study, by using the classical thin shell theory, an approximate solution, which was proposed by Agamirov (1990) and was used by Sofiyev (2010) for truncated conical shells, the authors tried to give analytical solutions to the problem of nonlinear stability analysis of FGM thin annular spherical shells on elastic foundations under uniform external pressure and temperature.

2. Governing equations

Consider an annular spherical shell made of FGM resting on elastic foundations with radius of curvature R, base radii r_1,r_0 and thickness h. The FGM annular spherical shell is subjected to external pressure q uniformly distributed on the outer surface as shown in Fig. 1.

The annular spherical shell is made from a mixture of ceramics and metals, and is defined in coordinate system (φ,θ,z), where φ and θ are in the meridional and circumferential direction of the shells, respectively and z is perpendicular to the middle surface positive inwards.

Suppose that the material composition of the shell varies smoothly along the thickness by a simple power law in terms of the volume fractions of the constituents as

$$V_c(z) = \left(\frac{2z+h}{2h}\right)^k, \quad -\frac{h}{2} \le z \le \frac{h}{2}, \qquad V_m(z) = 1 - V_c(z). \tag{1}$$

where k (volume fraction index) is a non-negative number that defines the material distribution, subscripts m and c represent the metal and ceramic constituents, respectively.

The effective properties of FGM shallow spherical shell such as modulus of elasticity, the coefficient of thermal expansion, the coefficient of thermal conduction of FGM annular spherical shell can be defined as

$$[E(z),\alpha(z),K(z)] = [E_m,\alpha_m,K_m] + [E_{cm},\alpha_{cm},K_{cm}]\left(\frac{2z+h}{2h}\right)^k, \quad -\frac{h}{2} \le z \le \frac{h}{2}. \tag{2}$$

The Poisson ratio ν is assumed to be constant $\nu(z) = const$ and $E_{cm} = E_c - E_m$, $\alpha cm = \alpha c - \alpha m$, $Kcm = Kc - Km$.

The reaction–deflection relation of Pasternak foundation is given by Dumir (1985) amd Duc et al. (2014).

$$q_e = k_1 w - k_2 \Delta w$$

where $\Delta w = \frac{\partial^2 w}{\partial r^2} + \frac{1}{r}\frac{\partial w}{\partial r} + \frac{1}{r^2}\frac{\partial^2 w}{\partial \theta^2}$ is a Laplace's operator, w is the deflection of the annular spherical shell, k_1 is Winkler foundation modulus and k_2 is the shear layer foundation stiffness of Pasternak model.

In the present study, the classical shell theory is used to obtain the equilibrium and compatibility equations as well as expressions of buckling loads and nonlinear load-deflection curves of thin FGM annular spherical shells. For a thin annular spherical shell it is convenient to introduce a variable r, referred as the radius of parallel circle with the base of shell and defined by $r = R\sin\varphi$. Moreover, due to shallowness of the shell it is approximately assumed that $\cos\varphi = 1$, $Rd\varphi = dr$.

According to the classical shell theory, the strains at the middle surface and the change of curvatures and twist are related to the displacement components u,v,w in the φ,θ,z coordinate directions, respectively, taking into account Von Karman–Donnell nonlinear terms as (Bich and Tung, 2011; Dumir, 1985; Xu, 1991; Duc et al., 2014).

$$\varepsilon_r^0 = \frac{\partial u}{\partial r} - \frac{w}{R} + \frac{1}{2}\left(\frac{\partial w}{\partial r}\right)^2, \qquad \chi_r = \frac{\partial^2 w}{\partial r^2},$$

$$\varepsilon_\theta^0 = \frac{1}{r}\frac{\partial v}{\partial \theta} + \frac{u}{R} - \frac{w}{R} + \frac{1}{2r^2}\left(\frac{\partial w}{\partial \theta}\right)^2, \qquad \chi_\theta = \frac{1}{r}\frac{\partial w}{\partial r} + \frac{1}{r^2}\frac{\partial^2 w}{\partial \theta^2}, \tag{3}$$

$$\gamma_r^\theta = \frac{\partial v}{\partial r} + \frac{1}{r}\frac{\partial u}{\partial \theta} - \frac{v}{r} + \frac{1}{r}\frac{\partial w}{\partial r}\frac{\partial w}{\partial \theta}, \qquad \chi_{r\theta} = \frac{1}{r}\frac{\partial^2 w}{\partial r \partial \theta} - \frac{1}{r^2}\frac{\partial w}{\partial \theta}.$$

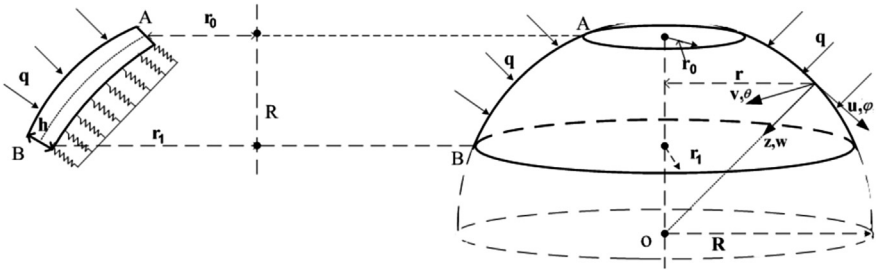

Fig. 1. Configuration of a FGM annular spherical shell.

where ε_r^0 and ε_θ^0 are the normal strains, γ_r^θ is the shear strain at the middle surface of the spherical shell, $\chi_r,\chi_\theta,\chi_{r\theta}$ are the changes of curvatures and twist.

The strains across the shell thickness at a distance z from the mid-plane are:

$$\varepsilon_r = \varepsilon_r^0 - z\chi_r \;;\; \varepsilon_\theta = \varepsilon_\theta^0 - z\chi_\theta \;;\; \gamma_{r\theta} = \gamma_r^\theta - z\chi_{r\theta}. \tag{4}$$

Using Eqs. (3) and (4), the geometrical compatibility equation of a shallow spherical shell is written as (Bich and Tung, 2011; Duc et al., 2014).

$$\frac{1}{r^2}\frac{\partial^2\varepsilon_r^0}{\partial\theta^2} - \frac{1}{r}\frac{\partial\varepsilon_r^0}{\partial r} + \frac{1}{r^2}\frac{\partial}{\partial r}\left(r^2\frac{\partial\varepsilon_\theta^0}{\partial r}\right) - \frac{1}{r^2}\frac{\partial^2}{\partial r\partial\theta}\left(r\gamma_r^\theta\right) = -\frac{\Delta w}{r} + \chi_{r\theta}^2 - \chi_r\chi_\theta, \tag{5}$$

The stress–strain relationships for annular spherical shell including temperature effect are defined by the Hooke law

$$(\sigma_r,\sigma_\theta) = \frac{E(z)}{1-\nu^2}[(\varepsilon_r,\varepsilon_\theta) + \nu(\varepsilon_\theta,\varepsilon_r) - (1+\nu)\alpha\Delta T(1,1)],$$
$$\sigma_{r\theta} = \frac{E(z)}{2(1+\nu)}\gamma_{r\theta}. \tag{6}$$

where σ_r and σ_θ are the normal stress, $\sigma_{r\theta}$ is the shear stress at the middle surface of the spherical shell in spherical system coordinate and ΔT denotes the increments of temperature from a surface to another one of FGM annular spherical shell.

The force and moment resultants of an FGM spherical shell are expressed in terms of the stress components through the thickness as:

$$(N_{ij},M_{ij}) = \int_{-h/2}^{h/2}\sigma_{ij}(1,z)\mathrm{d}z,\; ij = (rr,\theta\theta,r\theta) \tag{7}$$

In case of $(i=j=r)$ or $(i=j=\theta)$ for simplicity denoted $N_{rr}=N_r$, $N_{\theta\theta}=N_\theta$, $M_{rr}=M_r$, $M_{\theta\theta}=M_\theta$.

By using Eqs. (4), (6) and (7) the constitutive relations can be given as

$$(N_r,M_r) = \frac{(E_1,E_2)}{1-\nu^2}\left(\varepsilon_r^0+\nu\varepsilon_\theta^0\right) + \frac{(E_2,E_3)}{1-\nu^2}(\chi_r+\nu\chi_\theta) - \frac{(\Phi_m,\Phi_b)}{1-\nu},$$
$$(N_\theta,M_\theta) = \frac{(E_1,E_2)}{1-\nu^2}\left(\varepsilon_\theta^0+\nu\varepsilon_r^0\right) + \frac{(E_2,E_3)}{1-\nu^2}(\chi_\theta+\nu\chi_r) - \frac{(\Phi_m,\Phi_b)}{1-\nu},$$
$$(N_{r\theta},M_{r\theta}) = \frac{(E_1,E_2)}{2(1+\nu)}\gamma_{r\theta}^0 + \frac{(E_2,E_3)}{1+\nu}\chi_{r\theta}. \tag{8}$$

From the relations one can write

$$\varepsilon_r^0 = \frac{1}{E_1}\left(N_r-\nu N_\theta\right) + \frac{E_2}{E_1}\chi_r + \frac{\Phi_m}{E_1},$$
$$\varepsilon_\theta^0 = \frac{1}{E_1}\left(N_\theta-\nu N_r\right) + \frac{E_2}{E_1}\chi_\theta + \frac{\Phi_m}{E_1},$$
$$\gamma_{r\theta}^0 = \frac{2(1+\nu)}{E_1}N_{r\theta} + \frac{2E_2}{E_1}\chi_{r\theta},$$
$$M_r = \frac{E_2}{E_1}N_r - D(\chi_r+\nu\chi_\theta) - \frac{\Phi_b}{1-\nu},$$
$$M_\theta = \frac{E_2}{E_1}N_\theta - D(\chi_\theta+\nu\chi_r) - \frac{\Phi_b}{1-\nu},$$
$$M_{r\theta} = \frac{E_2}{E_1}N_{r\theta} - D\left(1-\nu\right)\chi_{r\theta}. \tag{9,10}$$

where:

$$E_1 = \int_{-h/2}^{h/2}\left[E_c + E_{cm}\left(\frac{2z+h}{h}\right)^k\right]\mathrm{d}z = hE_m + \frac{hE_{cm}}{k+1},$$
$$E_2 = \int_{-h/2}^{h/2} z\left[E_c + E_{cm}\left(\frac{2z+h}{h}\right)^k\right]\mathrm{d}z = h^2E_{cm}\left(\frac{1}{k+2} - \frac{1}{2k+2}\right),$$
$$E_3 = \int_{-h/2}^{h/2} z^2\left[E_c + E_{cm}\left(\frac{2z+h}{h}\right)^k\right]\mathrm{d}z = \frac{h^3E_m}{12} + \frac{h^3E_{cm}}{2(k+1)(k+2)(k+3)},$$
$$(\Phi_m,\Phi_b) = \int_{-h/2}^{h/2}\left[E_c + E_{cm}\left(\frac{2z+h}{h}\right)^k\right] \times\left[\alpha_c + \alpha_{cm}\left(\frac{2z+h}{h}\right)^k\right]\Delta T(1,z)\mathrm{d}z, \quad D = \frac{E_1E_3-E_2^2}{E_1\left(1-\nu^2\right)}. \tag{11}$$

The nonlinear equilibrium equations of a perfect shallow spherical shell based on the classical shell theory (Xu, 1991; Muc, 1992)

$$\frac{\partial N_r}{\partial r} + \frac{1}{r}\frac{\partial N_{r\theta}}{\partial\theta} + \frac{N_r}{r} - \frac{N_\theta}{r} = 0, \tag{12}$$

$$\frac{\partial N_\theta}{r\partial\theta} + \frac{\partial N_{r\theta}}{\partial r} + \frac{2N_{r\theta}}{r} = 0, \tag{13}$$

$$\frac{\partial^2 M_r}{\partial r^2} + \frac{2}{r}\frac{\partial M_r}{\partial r} + 2\left(\frac{\partial^2 M_{r\theta}}{r\partial r\partial\theta} + \frac{1}{r^2}\frac{\partial M_{r\theta}}{\partial\theta}\right) + \frac{1}{r^2}\frac{\partial^2 M_\theta}{\partial\theta^2} - \frac{1}{r}\frac{\partial M_\theta}{\partial r} + \frac{1}{R}(N_r+N_\theta) + \frac{1}{r}\frac{\partial}{\partial r}\left(rN_r\frac{\partial w}{\partial r} + N_{r\theta}\frac{\partial w}{\partial\theta}\right) + \frac{1}{r}\frac{\partial}{\partial\theta}\left(N_{r\theta}\frac{\partial w}{\partial r} + \frac{N_\theta}{r}\frac{\partial w}{\partial\theta}\right) + q - k_1w + k_2\Delta w = 0. \tag{14}$$

The Eqs. (12) and (13) are identically satisfied by introducing a stress function F as

$$N_r = \frac{1}{r}\frac{\partial F}{\partial r} + \frac{1}{r^2}\frac{\partial^2 F}{\partial\theta^2},\;\; N_\theta = \frac{\partial^2 F}{\partial r^2},\;\; N_{r\theta} = -\frac{1}{r}\frac{\partial^2 F}{\partial r\partial\theta} + \frac{1}{r^2}\frac{\partial F}{\partial\theta}. \tag{15}$$

Substituting Eqs. (3), (9) and (15) into the Eq. (5) and substituting Eqs. (3), (10) and (15) into Eq. (14) leads to

$$\frac{1}{E_1}\Delta\Delta F = -\frac{\Delta w}{R} + \left(\frac{1}{r}\frac{\partial^2 w}{\partial r\partial\theta} - \frac{1}{r^2}\frac{\partial w}{\partial\theta}\right)^2 - \frac{\partial^2 w}{\partial r^2}\left(\frac{1}{r}\frac{\partial w}{\partial r} + \frac{1}{r^2}\frac{\partial^2 w}{\partial\theta^2}\right), \tag{16}$$

$$D\Delta\Delta w - \frac{\Delta F}{R} - \left(\frac{1}{r}\frac{\partial F}{\partial r} + \frac{1}{r^2}\frac{\partial^2 F}{\partial^2\theta}\right)\frac{\partial^2 w}{\partial r^2} - \left(\frac{1}{r}\frac{\partial w}{\partial r} + \frac{1}{r^2}\frac{\partial^2 w}{\partial\theta^2}\right)\frac{\partial^2 F}{\partial r^2} + 2\left(\frac{1}{r}\frac{\partial^2 F}{\partial r\partial\theta} - \frac{1}{r^2}\frac{\partial F}{\partial\theta}\right)\left(\frac{1}{r}\frac{\partial^2 w}{\partial r\partial\theta} - \frac{1}{r^2}\frac{\partial w}{\partial\theta}\right) = q - k_1w + k_2\Delta w. \tag{17}$$

Regularly, the stress function F should be determined by the substitution of deflection function w into compatibility equation (16) and solving resulting equation. However, such a procedure is

very complicated in mathematical treatment because obtained equation is a variable coefficient partial differential equation. Accordingly, integration to obtain exact stress function $F(r,\theta)$ is extremely complex. Similarly, the problem of solving the equilibrium is in the same situation. Therefore one should find a transformation to lead Eqs. 16 and 17 into constant coefficient differential equations. Suppose such a transformation.

$$w = w(\varsigma), F = F_0(\varsigma)e^{2\varsigma}, \quad \text{where } r = r_0 e^{\varsigma}; \varsigma = \ln\frac{r}{r_0} \tag{18}$$

Substituting Eq. (18) into Eqs. 16 and 17 and establishing a lot of calculations lead to the transformed equations.

$$\begin{aligned}&\frac{1}{E_1}\left(\frac{\partial^4 F_0}{\partial\varsigma^4}+4\frac{\partial^3 F_0}{\partial\varsigma^3}+4\frac{\partial^2 F_0}{\partial\varsigma^2}+4\frac{\partial^3 F_0}{\partial\varsigma\partial\theta^2}+2\frac{\partial^4 F_0}{\partial\varsigma^2\partial\theta^2}+4\frac{\partial^2 F_0}{\partial\theta^2}+\frac{\partial^4 F_0}{\partial\theta^4}\right)\\&=-\frac{r_0^2}{R}\left(\frac{\partial^2 w}{\partial\varsigma^2}+\frac{\partial^2 w}{\partial\theta^2}\right)+\frac{1}{e^{4\varsigma}}\left(\frac{\partial^2 w}{\partial\varsigma\partial\theta}-\frac{\partial w}{\partial\theta}\right)^2+\frac{1}{e^{4\varsigma}}\left(\frac{\partial^2 w}{\partial\varsigma^2}-\frac{\partial w}{\partial\varsigma}\right)\\&\quad\times\left(\frac{\partial w}{\partial\varsigma}+\frac{\partial^2 w}{\partial\theta^2}\right);\end{aligned} \tag{19}$$

$$\begin{aligned}&D\left(\frac{\partial^4 w}{\partial\varsigma^4}-4\frac{\partial^3 w}{\partial\varsigma^3}+4\frac{\partial^2 w}{\partial\varsigma^2}-4\frac{\partial^3 w}{\partial\varsigma\partial\theta^2}+2\frac{\partial^4 w}{\partial\varsigma^2\partial\theta^2}+4\frac{\partial^2 w}{\partial\theta^2}+\frac{\partial^4 w}{\partial\theta^4}\right)+\\&-\frac{r_0^2 e^{4\varsigma}}{R}\left(\frac{\partial^2 F_0}{\partial\varsigma^2}+4\frac{\partial F_0}{\partial\varsigma}+4F_0+\frac{\partial^2 F_0}{\partial\theta^2}\right)\\&-\left(\frac{\partial F_0}{\partial\varsigma}+2F_0+\frac{\partial^2 F_0}{\partial\theta^2}\right)\left(\frac{\partial^2 w}{\partial\varsigma^2}-\frac{\partial w}{\partial\varsigma}\right)e^{2\varsigma}+\\&-\left(\frac{\partial^2 F_0}{\partial\varsigma^2}+2F_0+3\frac{\partial F_0}{\partial\varsigma}\right)\left(\frac{\partial w}{\partial\varsigma}+\frac{\partial^2 w}{\partial\varsigma\partial\theta}\right)e^{2\varsigma}\\&+2\left(\frac{\partial^2 F_0}{\partial\varsigma\partial\theta}+\frac{\partial F_0}{\partial\theta}\right)\left(\frac{\partial^2 w}{\partial\varsigma\partial\theta}-\frac{\partial w}{\partial\theta}\right)e^{2\varsigma}+\\&-qr_0^4e^{4\varsigma}+k_1wr_0^4e^{4\varsigma}-k_2\left(\frac{\partial^2 w}{\partial\varsigma^2}+\frac{\partial^2 w}{\partial\theta^2}\right)r_0^2e^{2\varsigma}=0.\end{aligned} \tag{20}$$

Eqs. (19) and (20) are the basic equations used to investigate the nonlinear buckling of FGM annular spherical shells. These are nonlinear equations in terms of two dependent unknowns $w(\varsigma)$ and $F_0(\varsigma)$.

3. Stability analysis

In this section, an analytical approach is used to investigate the nonlinear stability analysis of FGM annular spherical shell under mechanical loads including the effects of temperature. The FGM annular spherical shell is assumed to be simply supported along the periphery and subjected to mechanical loads uniformly distributed on the outer surface and the base edges of the shell. Depending on the in-plane behavior at the edge of boundary conditions will be considered in case the edges are simply supported and immovable. For this case, the boundary conditions are

$$u = 0,\ \ w = 0,\ \ \frac{\partial^2 w}{\partial\varsigma^2}-\frac{\partial w}{\partial\varsigma}=0,\ \ N_r = N_0,\ \ N_{r\theta}=0,\ \ \text{with } \varsigma = 0\ \ (\text{i.e at } r = r_0). \tag{21}$$

where N_0 is the fictitious compressive load rendering the immovable edges.

The boundary conditions (21) can be satisfied when the deflection w is approximately assumed as follows (Agamirov, 1990; Sofiyev, 2010)

$$w = We^{\varsigma}\sin(\beta_1\varsigma)\sin(n\theta),\ \ \beta_1 = \frac{m\pi}{a},\ \ a = \ln\frac{r_1}{r_0} \tag{22}$$

where W is the maximum amplitude of deflection and m,n are the numbers of half waves in meridional and circumferential direction, respectively. The form of this approximate solution was proposed by Agamirov (1990) and it was used by Sofiyev (2010) for FGM truncated conical shells.

Introduction of Eq. (22) into Eq. (19) gives

$$\begin{aligned}&\frac{1}{E_1}\left(\frac{\partial^4 F_0}{\partial\varsigma^4}+4\frac{\partial^3 F_0}{\partial\varsigma^3}+4\frac{\partial^2 F_0}{\partial\varsigma^2}+4\frac{\partial^3 F_0}{\partial\varsigma\partial\theta^2}+2\frac{\partial^4 F_0}{\partial\varsigma^2\partial\theta^2}+4\frac{\partial^2 F_0}{\partial\theta^2}+\frac{\partial^4 F_0}{\partial\theta^4}\right)=\\&-\frac{r_0^2e^{\varsigma}W}{R}\left[\left(1-\beta_1^2-n^2\right)\sin(\beta_1\varsigma)+2\beta_1\cos(\beta_1\varsigma)\right]\sin(n\theta)\\&+\frac{W^2\beta_1^2}{2}(n^2-1)\cos(2\beta_1\varsigma)-\frac{W^2}{4}\left(\beta_1-\beta_1 n-\beta_1^3\right)\sin(2\beta_1\varsigma)\\&+\frac{W^2}{2}\beta_1^2n^2\cos(2n\theta)+\frac{W^2}{4}\left(\beta_1-\beta_1n^2-\beta_1^3\right)\sin(2\beta_1\varsigma)\cos(2n\theta)\\&+\frac{W^2}{2}\beta_1^2\cos(2\beta_1\varsigma)\cos(2n\theta).\end{aligned} \tag{23}$$

Solving this obtained equation with the boundary conditions (21) for the stress function F_0 yields

$$\begin{aligned}F_0 =\ &f_1e^{\varsigma}\sin(\beta_1\varsigma)\sin(n\theta)+f_2e^{\varsigma}\cos(\beta_1\varsigma)\sin(n\theta)+f_3\cos(2\beta_1\varsigma)\\&+f_4\cos(2n\theta)+f_5\cos(2\beta_1\varsigma)\cos(2\beta_2\theta)\\&+f_6\sin(2\beta_1\varsigma)\cos(2n\theta)+f_7\sin(2\beta_1\varsigma)+\frac{1}{2}N_0r_0^2.\end{aligned} \tag{24}$$

where

$$\begin{aligned}f_1 &= -\frac{r_0^2E_1W\left[A\left(1-\beta_1^2-n^2\right)+2B\beta_1\right]}{\left(A^2+B^2\right)R},\\f_2 &= -\frac{r_0^2E_1W\left[B\left(1-\beta_1^2-n^2\right)+2A\beta_1\right]}{\left(A^2+B^2\right)R},\\f_3 &= E_1l_3W^2,\\f_4 &= E_1l_4W^2, f_5 = E_1l_4W^2\ \ , f_6 = E_1l_6W^2\ \ , f_7 = E_1l_7W^2,\end{aligned} \tag{25}$$

and

$$\begin{aligned}&A = 9-22\beta_1^2+\beta_1^4+n^4-10n^2+2\beta_1^2n^2, B = 8\beta_1^3-24\beta_1+8\beta_1n^2,\\&l_3 = \frac{b_6c_3+c_4a_6}{a_3b_6+a_6b_3},\ \ l_4 = \frac{\beta_1^2}{32\left(\beta_2^2-1\right)},\ \ l_5 = \frac{b_5c_5+a_5c_6}{a_4b_5+a_5b_4},\\&l_6 = \frac{a_4c_6-b_4c_5}{a_4b_5+a_5b_4},\ \ l_7 = \frac{a_3c_4-b_3c_3}{a_3b_6+a_6b_3},\end{aligned} \tag{26}$$

The remaining constants are given in Appendix I.

After substitution Eqs. (22) and (24) in Eq. (20), for simplicity, the left hand side of the last obtained equation is denoted by Φ. Applying Galerkin method with the limits of integral is given by the formula

$$\int_0^{\ln\frac{r_1}{r_0}}\int_0^{2\pi}\Phi e^{\varsigma}\sin(\beta_1\varsigma)\sin(n\theta)\mathrm{d}\varsigma\mathrm{d}\theta = 0, \tag{27}$$

we obtain the following equation

$$q-\frac{N_0A_5}{B_1r_0^2}W-\frac{A_0N_0}{RB_1}=\left(\frac{DA_3}{B_1r_0^4}+\frac{E_1A_4}{B_1R^2}+\frac{k_1A_6}{B_1}+\frac{k_2A_7}{B_1r_0^2}\right)W+\frac{E_1A_2}{RB_1r_0^2}W^2+\frac{E_1A_1}{B_1r_0^4}W^3. \quad (28)$$

where the constants $B_1,A_0,A_1,A_2,A_3,A_4,A_5,A_6,A_7$ are given in Appendix II.

Eq. (28) is used to determine the buckling loads and nonlinear equilibrium paths of FGM annular spherical shell under uniform external pressure with and without the effects of temperature conditions.

3.1. Mechanical stability analysis

The simply supported FGM annular spherical shell with freely movable edge is assumed to be subjected to external pressure q (in Pascals) uniformly distributed on the outer surface of the shell in the absence of temperature conditions. In this case $N_0=0$ and Eq. (28) reduces to

$$q=\left(\frac{D^*R_h^4A_3}{B_1R_0^4}+\frac{E_1^*A_4R_h^2}{B_1}+\frac{K_1D^*A_6}{B_1}+\frac{K_2D^*A_7R_h^2}{B_1R_0^2}\right)W^*+\frac{E_1^*A_2R_h^3}{B_1R_0^2}(W^*)^2+\frac{E_1^*A_1R_h^4}{B_1R_0^4}(W^*)^3 \quad (29)$$

where, by putting

$$E_1^*=\frac{E_1}{h},\ E_2^*=\frac{E_2}{h^2},\ W^*=\frac{W}{h},\ R_h=\frac{h}{R};\ R_0=\frac{r_0}{R};\ D^*=\frac{D}{h^3};\ K_1=\frac{k_1h^4}{D};\ K_2=\frac{k_2h^2}{D}.$$

If the FGM annular spherical shell does not rest on elastic foundations ($K_1=K_2=0$), we received:

$$q=\left(\frac{D^*R_h^4A_3}{B_1R_0^4}+\frac{E_1^*A_4R_h^2}{B_1}\right)W^*+\frac{E_1^*A_2R_h^3}{B_1R_0^2}(W^*)^2+\frac{E_1^*A_1R_h^4}{B_1R_0^4}(W^*)^3. \quad (30)$$

Eq. (30) may be used to find static critical buckling load and trace postbuckling load-deflection curves of FGM annular spherical shell. It is evident $q(W^*)$ curves originate from the coordinate origin. In addition, Eq. (29) indicates that there is no bifurcation − type buckling for pressure loaded annular spherical shell and extremum − type buckling only occurs under definite conditions.

The extremum pressure buckling load of the shell can be found from Eq. (29) using the condition $\frac{dq}{dW^*}=0$.

3.2. Thermomechanical stability analysis

A FGM annular spherical shell simply supported with immovable edges under simultaneous action of uniform external pressure q and temperature is considered.

The condition expressing the immovability on the boundary edges, i.e. $u=0$ on $r=r_0$, and $r=r_1$ is fulfilled on the average sense as

$$\int_0^{\pi}\int_{r_0}^{r_1}\frac{\partial u}{\partial r}r\,dr\,d\theta=0. \quad (31)$$

From Eqs. (3) and (9) one can obtain the following relation

$$\frac{\partial u}{\partial r}=\varepsilon_r^0+\frac{w}{R}-\frac{1}{2}\left(\frac{\partial w}{\partial r}\right)^2=\frac{1}{E_1}\left(\frac{1}{r}\frac{\partial F}{\partial r}+\frac{1}{r^2}\frac{\partial^2F}{\partial\theta^2}-\nu\frac{\partial^2F}{\partial r^2}\right)+\frac{E_2}{E_1}\frac{\partial^2w}{\partial r^2}+\frac{\Phi_m}{E_1}+\frac{w}{R}-\frac{1}{2}\left(\frac{\partial w}{\partial r}\right)^2. \quad (32)$$

Using the transformation (18) into Eq. (32) yields

$$\frac{\partial u}{\partial r}=\frac{1}{E_1r_0^2}\left[\frac{\partial F_0}{\partial\varsigma}+2F_0+\frac{\partial^2F_0}{\partial\theta^2}-\nu\left(\frac{\partial^2F_0}{\partial\varsigma^2}+3\frac{\partial F_0}{\partial\varsigma}+2F_0\right)\right]+\frac{E_2}{E_1r_0^2e^{2\varsigma}}\left(\frac{\partial^2w}{\partial\varsigma^2}-\frac{\partial w}{\partial\varsigma}\right)++\frac{\Phi_m}{E_1}+\frac{w}{R}-\frac{1}{2r_0^2e^{2\varsigma}}\left(\frac{\partial w}{\partial\varsigma}\right)^2. \quad (33)$$

Introduction of Eqs. 22 and 24 into the Eq. (33) then substituting obtained result into Eq. (31) lead to the expression for the fictitious load N_0 (where the constants A_8,A_9,A_{10} are given in Appendix II.)

$$N_0=\frac{-\Phi_m}{(1-\nu)}+\frac{E_1}{(-1+\nu)(-1+e^{2a})\pi r_0^2}\left[\frac{E_2A_9}{E_1}+\frac{r_0^2A_{10}}{R}\right]W+\frac{E_1A_8}{(-1+\nu)(-1+e^{2a})\pi r_0^2}W^2 \quad (34)$$

which represents the fictitious compressive stress making the edges immovable.

Specific expressions of parameter Φ_m in two cases of thermal loading will be determined.

3.2.1. Uniform temperature rise

Environment temperature is assumed to be uniformly raised from initial value T_i at which the shell is thermal stress free, to final one T_f and temperature change ($\Delta T=T_f-T_i$) is independent to thickness variable (Bich and Tung, 2011). The thermal parameter Φ_m can be expressed in terms of the ΔT: $\Phi_m=Ph\Delta T$. Subsequently, employing this expression Φ_m in Eq. (34) and then substitution of the result N_0 into Eq. (28) lead to

$$q=\frac{-A_0P\Delta TR_h}{(1-\nu)B_1}-\frac{P\Delta TA_5R_h^2}{(1-\nu)B_1R_0^2}W^*+\left[\frac{D^*R_h^4A_3}{B_1R_0^4}+\frac{E_1^*A_4R_h^2+K_1D^*A_6}{B_1}+\frac{K_2D^*A_7R_h^2}{B_1R_0^2}+\frac{A_0\left(E_2^{*3}A_9R_h^3+R_0^2E_1^*A_{10}R_h^2\right)}{(-1+\nu)(-1+e^{2a})\pi B_1R_0^2}\right]W^*+\left[\frac{E_1^*A_2R_h^3}{B_1R_0^2}+\frac{\left(A_5A_9E_2^*R_h^4+E_1^*A_5A_{10}R_h^3R_0^2\right)}{(-1+\nu)(-1+e^{2a})\pi B_1R_0^4}+\frac{A_0E_1^*A_8R_h^3}{(-1+\nu)(-1+e^{2a})\pi B_1R_0^2}\right](W^*)^2+\left[\frac{E_1^*A_1R_h^4}{B_1R_0^4}+\frac{E_1^*A_5A_8R_h^4}{(-1+\nu)(-1+e^{2a})\pi R_0^4B_1}\right](W^*)^3 \text{ where : } P=E_c\alpha_c+\frac{E_c\alpha_{mc}+E_{mc}\alpha_c}{k+1}+\frac{E_{mc}\alpha_{mc}}{2k+1}. \quad (35)$$

Eq. (35) shows that when thermal load (ΔT) $\neq 0$ the deflection

curve $q(W^*)$ starting from a pressure point on the axis q defined by the term: $-A_0P\Delta TR_h/(1-\nu)B_1$.

3.2.2. Through the thickness temperature gradient

The metal-rich surface temperature T_m is maintained at stress free initial value while ceramic-rich surface temperature T_c is elevated and in this case, the temperature through the thickness is governed by the one-dimensional Fourier equation of steady-state heat conduction established in spherical coordinate system whose origin is the center of complete sphere as (Bich and Tung, 2011)

$$\frac{\mathrm{d}}{\mathrm{d}\bar{z}}\left[K(\bar{z})\frac{\mathrm{d}T}{\mathrm{d}\bar{z}}\right]+\frac{2K(\bar{z})\mathrm{d}T}{\bar{z}\mathrm{d}\bar{z}}=0;\quad T\Big|_{\bar{z}=R-\frac{h}{2}}=T_m;\quad T\Big|_{\bar{z}=R+\frac{h}{2}}=T_c; \tag{36}$$

where $\bar{z}$ is radial coordinate of a point which is distant z from the shell middle surface with respect to the center of sphere, i.e., $\bar{z}=R+z$ and $R-h/2\le\bar{z}\le R+h/2$.

The solution of Eq. (36) can be obtained as follows.

$$T(\bar{z})=T_m+\frac{\Delta T}{\int_{R-\frac{h}{2}}^{R+\frac{h}{2}}\frac{\mathrm{d}\bar{z}}{\bar{z}^2K(\bar{z})}}\int_{R-\frac{h}{2}}^{\bar{z}}\frac{\mathrm{d}\tau}{\tau^2K(\tau)} \tag{37}$$

where, in this case of thermal loading, $\Delta T=T_c-T_m$ is the temperature difference between ceramic-rich and metal-rich surfaces of the FGM spherical shell. Due to mathematical difficulty, this section only considers linear distribution of metal and ceramic constituents, i.e. $k=1$, and

$$K(\bar{z})=K_m+K_{cm}\frac{2(\bar{z}-R)+h}{2h}. \tag{38}$$

Substituting Eq. (38) into Eq. (37) gives temperature distribution across the shell thickness as

$$T(z)=T_m+\frac{\Delta T}{I}\left\{\frac{4K_{cm}}{(K_c+K_m-2K_{cm}R_h)^2h}\left[\ln\frac{(K_c+K_m)h+2K_{cm}z}{2hK_m}-\ln\frac{2(R+z)}{2R-h}\right]+\frac{2(2z+h)}{(K_c+K_m-2K_{cm}R_h)(R+z)2R-h}\right\} \tag{39}$$

where $\bar{z}$ has been replaced by $z+R$ after integration.

Assuming the metal surface temperature as reference temperature and substituting Eq. (39) into Eq. (11) give $\Phi_m=\frac{h\Delta TL}{I}$.

The explicit analytical expressions of L,I are calculated and given in the Appendix.

By following the same procedure as the preceding loading case we obtain thermo-mechanical $q(W^*)$ curves for the case of through the thickness temperature gradient as Eq. (35) provided is replaced by L/I. Such an expression is omitted here for sake of brevity.

4. Results and discussion

In this section, the nonlinear response of the FGM annular spherical shell is analyzed. The shell is assumed to be simply supported along boundary edges and, unless otherwise specified, edges are freely movable. In characterizing the behavior of the spherical shell, deformations in which the central region of a shell moves toward the plane that contains the periphery of the shell are referred to as inward deflections (positive deflections). Deformations in the opposite direction are referred to as outward deflection (negative deflections).

The following properties of the FGM shell are chosen (Bich and Tung, 2011; Duc et al., 2014):

$$E_m=70\ \text{GPa},\quad \alpha_m=23\times10^{-6}\,{}^\circ C^{-1},\quad K_m=204\text{W/mK};$$
$$E_c=380\ \text{GPa}\quad \alpha_m=7.4\times10^{-6}\,{}^\circ C,\quad K_m=10.4\text{W/mK}.$$

where Poisson's ratio is chosen to be $\nu=0.3$.

The effects of material and geometric parameters on the nonlinear response of the FGM annular spherical shells under mechanical loads (without effect temperature and elastic foundations$K_1=K_2=0$) are presented in Figs. 2–5. It is noted that in all figures W/h denotes the dimensionless maximum deflection of the shell.

Fig. 2 shows the effects of volume fraction index k(0,1,5,+∞) on the nonlinear response of the FGM annular spherical shell subjected to external pressure (mode(m,n) = (1,11)). As can be seen, the load-deflection curves become lower when k increases. This is expected because the volume percentage of ceramic constituent, which has higher elasticity modulus, is dropped with increasing values of k.

Fig. 3 depicts the effects of curvature radius − thickness ratio R/h (200, 300, 400, and 500) on the nonlinear behavior of the external pressure of the FGM annular spherical shells (mode (m,n) = (1,11)). From Fig. 3 we can conclude that when the annular spherical shells get thinner − corresponding with R/h getting bigger, the critical buckling loads will get smaller.

Fig. 4 analyzes the effects of 2 base-curvature radius ratio r_1/r_0 on the nonlinear response of FGM annular spherical shells subjected to uniform external pressure. It is shown that the nonlinear response of annular spherical shells is very sensitive with change of r_1/r_0 ratio characterizing the shallowness of annular spherical shell. Specifically, the enhancement of the upper buckling loads and the load carrying capacity in small range of deflection as r_1/r_0 increases is followed by a very severe snap − through behaviors. In other words, in spite of possessing higher limit buckling loads, deeper spherical shells exhibit a very unstable response from the post-buckling point of view. Furthermore, in the same effects of base-curvature radius ratio r_1/r_0 the load of the nonlinear response of FGM annular spherical shells is higher when the shallowness of annular spherical shell (H) is smaller, where H is the distance between two radius r_1,r_0, and calculated by

$$H(r_1,r_0)=\sqrt{R^2-r_0^2}-\sqrt{R^2-r_1^2}=R\left[\sqrt{1-\left(\frac{r_0}{R}\right)^2}-\sqrt{1-\left(\frac{r_1}{R}\right)^2}\right]$$

Fig. 5 examines the dependence of the nonlinear response of FGM annular spherical shells on the mode (m,n). It is easily

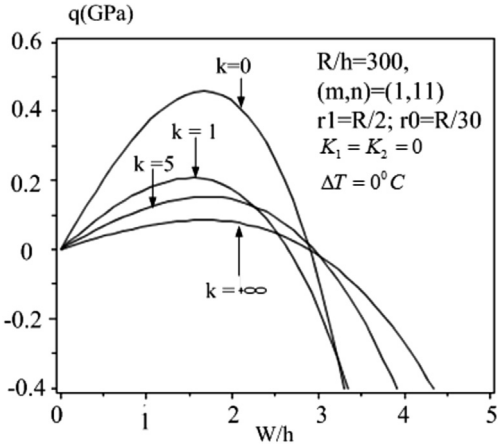

Fig. 2. Effects of volume fraction index k on the nonlinear response of the FGM annular spherical shell under external pressure.

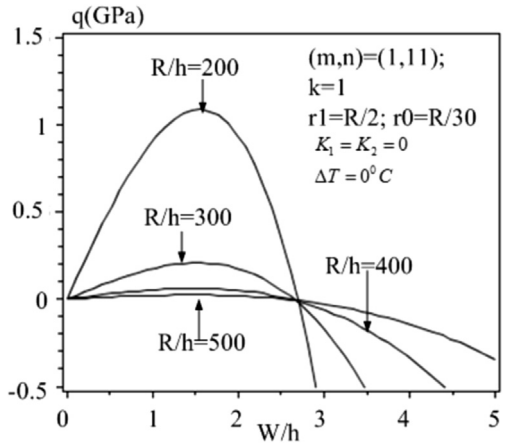

Fig. 3. Effects of curvature radius–thickness ratio on the nonlinear response of FGM annular spherical shells under external pressure.

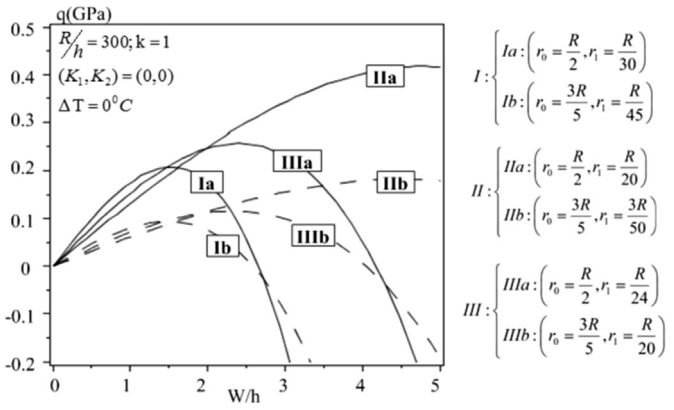

Fig. 4. Effects of radius of base–curvature radius ratio r_1/r_0 on the nonlinear response of FGM annular spherical shells.

recognized that with $m = 1$, the more increased the value of n, the higher increasing of the value of extreme point, corresponding to the higher load capacity of the shells. Note that, when m is even or $m \geq 3$, the graphic consists of symmetric curves through the origin of the coordinate system and the extreme point does not exist in the load-deflection curves.

The effects of temperature and elastic foundations on the nonlinear response of the FGM annular spherical shells under uniform external pressure are presented in Figs. 6–10.

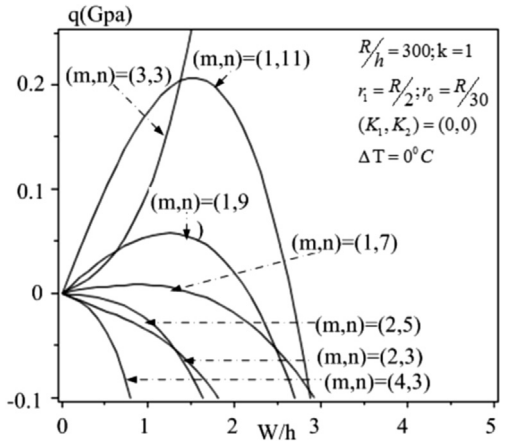

Fig. 5. Effects of mode (m,n) on the nonlinear response of FGM annular spherical shells.

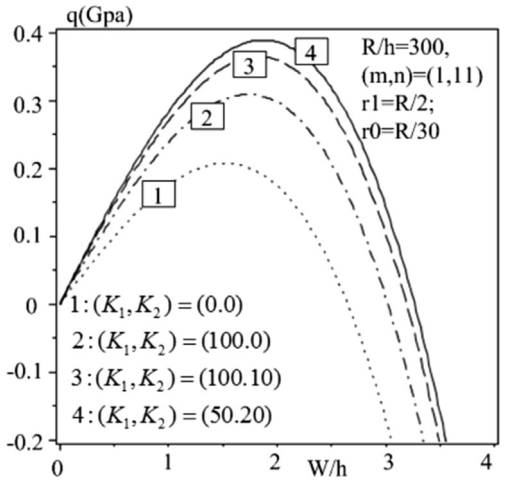

Fig. 6. Effects of the elastic foundations (K_1,K_2) on the nonlinear response of FGM annular spherical shells.

Effects of the elastic foundations (K_1,K_2) on the nonlinear response of FGM annular spherical shells are shown in Fig. 6. Obviously, elastic foundations played positive role on nonlinear static response of the FGM annular spherical shell: the large K_1 and K_2 coefficients are, the larger loading capacity of the shells is. It is clear that the elastic foundations can enhance the mechanical loading capacity for the FGM annular spherical shells, and the effect of Pasternak foundation K_2 on critical uniform external pressure is bigger than the Winkler foundation K_1.

Fig. 7 presents the effects of temperature and elastic foundations on the nonlinear response of FGM annular spherical shells under uniform external pressure. As shown in Fig. 7, the temperature makes the annular spherical shell to be deflected outward prior to mechanical loads acting on it. Under mechanical loads, outward deflection of the shell is reduced, and external pressure exceeds bifurcation point of load, an inward deflection occurs. In this context, Fig. 7 also shows the bad effect of temperature on the nonlinear response of the FGM annular spherical shells. Indeed, the mechanical loading ability of the system has been reduced in the presence of temperature.

The effects of temperature gradient through the thickness on the nonlinear response of FGM annular spherical shells under uniform external pressure are shown in Fig. 8. In this case, the metal-rich

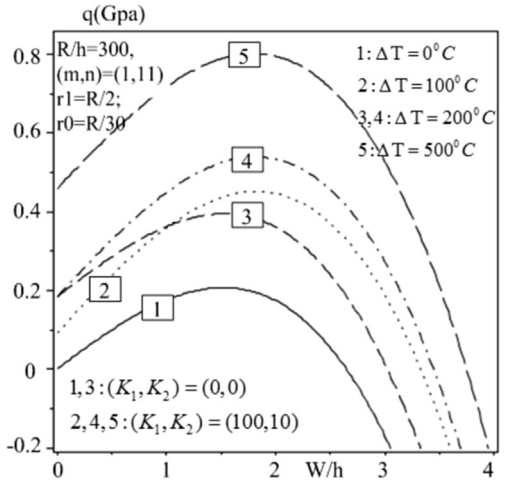

Fig. 7. Effects of uniform temperature rise and elastic foundations on the nonlinear response of FGM annular spherical shells.

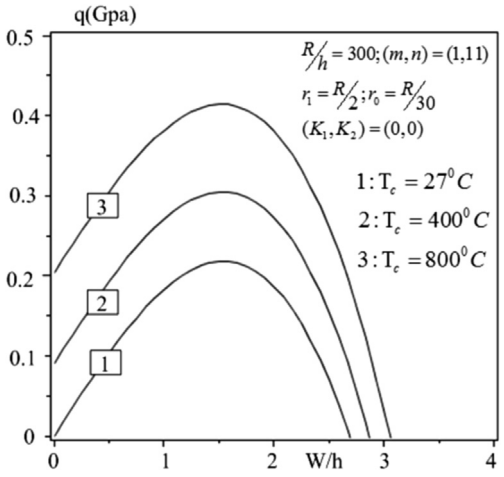

Fig. 8. Effects of temperature gradient on the nonlinear response of FGM annular spherical shell.

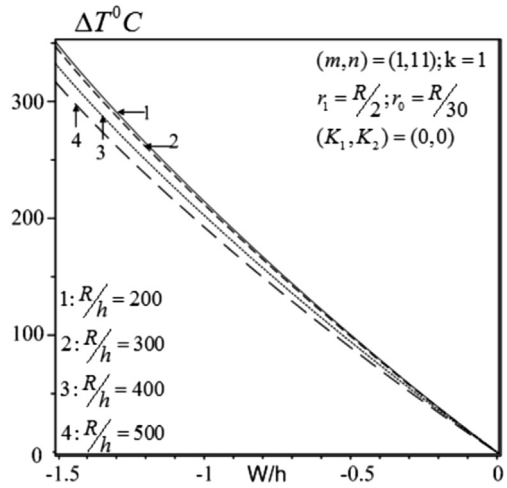

Fig. 10. Effects of curvature radius–thickness ratio on the thermal nonlinear response of FGM annular spherical shells.

surface temperature T_m is maintained at initial value $T_m = 27$ °C (room temperature) and temperature is transmitted from ceramic-rich surface through the thickness of annular. In Figs. 7 and 8, we can realize that the buckling load capacities of the shell in the cases of uniform temperature rise are better than the one in cases of gradient temperature through the thickness of the shell.

Fig. 9 shows the effects of volume fraction index k on the thermal nonlinear response of FGM annular spherical shells under uniform temperature rise. As can be observed, the annular spherical shells deflect outwards under thermal loads and the response of the annular spherical shells are relatively benign, i.e. there is no snap-through phenomenon and bifurcation type buckling.

Fig. 10 presents the effects of curvature radius-thickness ratio on the thermal nonlinear response of FGM annular spherical shells under uniform temperature rise. It is evident that the effects of curvature radius–thickness ratio on the thermal nonlinear response is not considerable, i.e. the thermal load-deflection curves approach contiguous when the ratio R/h changes.

Fig. 11 examines the dependence of the thermal nonlinear response of FGM annular spherical shells on the mode (m,n) in the presence of temperature. It is easily recognized that with $m = 1$, the more increased the value of n the higher increasing of the thermal nonlinear response.

Fig. 12 investigates the effects of the pre-existent external pressure on the thermal loading ability of the annular spherical shells in the presence of temperature. Shown in this figure is a monotonically increasing nonlinear response with outward deflection of the annular spherical shells. The annular spherical shells exhibit a bifurcation buckling behavior when they are subjected to external pressure prior to the application of thermal load. Both the bifurcation buckling loads and the capability of temperature resistance are enhanced with the increase in pre-existent uniform external pressure. However, with all values of mechanical load, the thermal postbuckling behavior is very stable, i.e. without a snap-through. In fact, the shell deflects inwards under external pressure and when temperature reaches a specific value, i.e. bifurcation point temperature, the shell surface returns to initial state. When the temperature exceeds bifurcation point, the spherical shell is monotonically deflected outwards.

5. Concluding remarks

Due to practical importance of FGM annular spherical shells and the lack of investigations on stability of these structures, the present paper aims to propose an analytical approach to study the

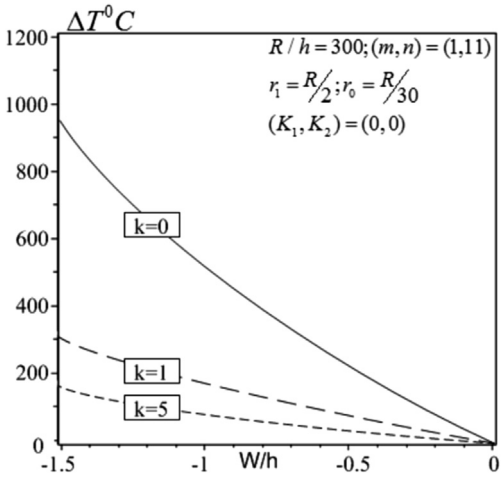

Fig. 9. Effects of volume fraction index k on the thermal nonlinear response of FGM annular spherical shells.

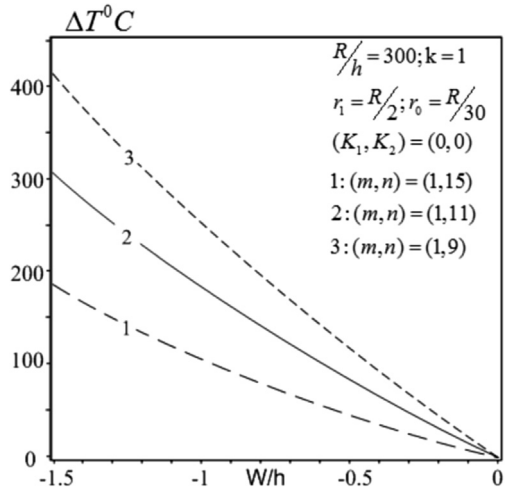

Fig. 11. Effects of mode (m,n) on the thermal nonlinear response of FGM annular spherical shells.

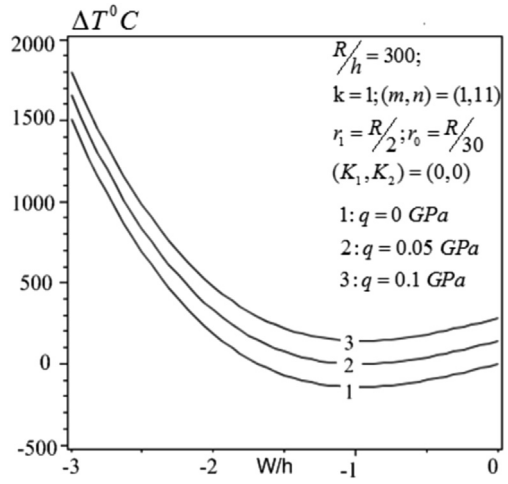

Fig. 12. Effects of pre-existent external pressure on the thermal nonlinear response of FGM shallow spherical shells.

problem of nonlinear stability analysis of FGM thin annular spherical shells on elastic foundations under uniform external pressure and temperature. Based on the classical shell theory, the equilibrium and compatibility equations are derived in terms of the shell deflection and the stress function. This system of equations has been transformed into another system of more simple equations. Galerkin method is used to get the explicit expression of postbuckling load-deflection curves of the shells. The effects of material, geometrical properties, elastic foundations and combination of external pressure and temperature on the nonlinear buckling and postbuckling of the FGM annular spherical shells are analyzed and discussed.

Acknowledgment

This paper was supported by the Grant in Mechanics *"Nonlinear analysis on stability and dynamics of functionally graded shells with special shapes"* code QG.14.02 of Vietnam National University, Hanoi. The authors are grateful for this support.

Appendix I

$$
\begin{aligned}
a_3 &= 16\left(\beta_1^4-\beta_1^2\right), & b_3 &= 32\beta_1^3,\\
a_4 &= 16\left(\beta_1^4-\beta_1^2+2\beta_1^2n^2-n^2+n^4\right), & b_4 &= 32\left(\beta_1^3+\beta_1n^2\right),\\
a_5 &= 32\left(\beta_1^3+\beta_1n^2\right), & b_5 &= 16\left(\beta_1-\beta_1^2+2\beta_1^2n^2-n^2+n^4\right),\\
a_6 &= 32\beta_1^3, & b_6 &= 16\left(\beta_1^4-\beta_1^2\right),\\
c_3 &= 0.5\left(\beta_1^2n^2-\beta_1^2\right), & c_5 &= 0.5\beta_1^2,\\
c_4 &= 0.25\left(\beta_1n^2-\beta_1+\beta_1^3\right), & c_6 &= -c_4,
\end{aligned}
$$

Appendix II

$$
C_1 = a_4,\ C_2 = b_5,\ B_1 = \frac{-2m\pi a\left(-1+e^{5a}(-1)^m\right)}{n\left(25a^2+m^2\pi^2\right)},
$$

$$
A_0 = \frac{m^2\pi^3\left(1-e^{6a}\right)}{\left(9a^2+m^2\pi^2\right)};
$$

$$
\begin{aligned}
A_1 =& h_{11}+h_{12}\left(\frac{m\pi}{a}t_3+t_4-2t_4n^2\right)+h_{13}\left(\frac{m\pi}{a}t_6+t_5\right)\\
&+h_{14}\left(\frac{m\pi}{a}t_5+t_6\right)+h_{15}\left(\frac{m\pi}{a}t_4-t_3-2t_3n^2\right)\\
&+h_{16}\left(\frac{2m^2\pi^2}{a^2}t_3+\frac{3m\pi}{a}t_4-t_3\right)\\
&+h_{17}\left(\frac{-2m^2\pi^2}{a^2}t_4+\frac{3m\pi}{a}t_3+t_4\right)\\
&+h_{18}\left(\frac{2m^2\pi^2}{a^2}t_5+\frac{3m\pi}{a}t_6-t_5\right)\\
&+h_{19}\left(\frac{-2m^2\pi^2}{a^2}t_6+\frac{3m\pi}{a}t_5+t_6\right)+h_{110}\left(t_3-\frac{2m\pi}{a}t_4\right)\\
&+h_{111}\left(t_4+\frac{2m\pi}{a}t_3\right),
\end{aligned}
$$

$$
\begin{aligned}
A_2 =& h_{21}\left(-6t_1+\frac{m^2\pi^2}{a^2}t_1+\frac{5m\pi}{a}t_2\right)\\
&+h_{22}\left(6t_2-\frac{m^2\pi^2}{a^2}t_2+\frac{5m\pi}{a}t_1\right)\\
&+h_{23}\left(-t_3+\frac{2m\pi}{a}t_4+\frac{m^2\pi^2}{a^2}t_3+n^2t_3\right)\\
&+h_{24}\left(t_3+\frac{2m\pi}{a}t_3-\frac{m^2\pi^2}{a^2}t_4+n^2t_4\right)\\
&+h_{25}\left(\frac{m^2\pi^2}{a^2}t_5+\frac{2m\pi}{a}t_6-t_5\right)\\
&+h_{26}\left(\frac{-m^2\pi^2}{a^2}t_6+\frac{2m\pi}{a}t_5+t_6\right)+h_{27}\\
&+h_{28}\left(2nt_1-\frac{mn\pi}{a}t_2\right)+h_{29}\left(2nt_2+\frac{mn\pi}{a}t_1\right)\\
&+h_{210}\left(-3t_1+\frac{m\pi}{a}t_2+n^2t_1\right)+h_{211}\left(3t_2+\frac{m\pi}{a}t_1-n^2t_2\right),
\end{aligned}
$$

$$A_3 = \frac{1}{8}\frac{m^2\pi^3(e^{2a}-1)(a^4+2m^2\pi^2a^2+m^4\pi^4-2n^2a^4+2m^2n^2\pi^2a^2+n^4a^4)}{a^4(a^2+m^2\pi^2)},$$

$$A_4 = \frac{-m^2\pi^3(e^{6a}-1)(-9t_1a^2+6t_2m\pi a+t_1m^2\pi^2+t_1n^2a^2)}{24a^2(9a^2+m^2\pi^2)} + \frac{m\pi^2(e^{6a}-1)(-9t_2a^2-6t_1m\pi a+t_2m^2\pi^2+t_2n^2a^2)}{8a(9a^2+m^2\pi^2)},$$

$$A_5 = \frac{-8m^3\pi^3(-3m^2\pi^2-7a^2+3e^{5a}m^2\pi^2(-1)^m+7e^{5a}(-1)^ma^2)}{3an(625a^4+250m^2\pi^2a^2+9m^4\pi^4)},$$

$$A_6 = \frac{m^2\pi^3(e^{6a}-1)}{24(9a^2+m^2\pi^2)};$$

$$A_7 = \frac{m^2\pi^3(-m^2\pi^2+3a^2e^{4a}-3a^2+e^{4a}m^2\pi^2)}{16a^2(4a^2+m^2\pi^2)};$$

$$A_8 = \left[\frac{m^2\pi^2}{16a^2} - \frac{(t_6a^2+t_5m\pi a-\nu t_6a^2+2\nu t_6m^2\pi^2-3\nu t_5m\pi a)}{a^2+m^2\pi^2} + \frac{m\pi(t_5a^2-t_6m\pi a-\nu t_5a^2+2\nu t_5m^2\pi^2+3\nu t_6m\pi a)}{a(a^2+m^2\pi^2)}\right];$$

$$A_9 = \frac{-\pi m(-1+e^a(-1)^m)}{an};$$

$$h_{13} = \frac{\pi^3m^2(e^{4a}-1)(2\pi m-a)}{16a(a^2+m^2\pi^2)} + \frac{9m^7n\pi^{10}(-1+e^{4a})^2}{16a(4a^4+5a^2m^2\pi^2+m^4\pi^4)};$$

$$h_{14} = -2h_{12};\quad h_{15} = -\frac{1}{2}h_{13};$$

$$h_{16} = \frac{-3a\pi^4m^3(-1+e^{2a})}{8(a^4+5a^2m^2\pi^2+4m^4\pi^4)} + \frac{\pi^3m^2(-1+e^{2a})}{4(a^2+4m^2\pi^2)};$$

$$h_{17} = \frac{\pi^2m(e^{2a}-1)[2\pi^3m^3-a^2\pi m+a^3+am^2\pi^2]}{8(a^2+4m^2\pi^2)(a^2+m^2\pi^2)};$$

$$h_{18} = \frac{\pi^3m^2(-1+e^{2a})(3a\pi m-2a^2-2\pi^2m^2)}{4(a^2+4m^2\pi^2)(a^2+m^2\pi^2)};$$

$$h_{19} = \frac{\pi^2m(e^{2a}-1)[-4\pi^3m^3+2a^2\pi m+a^3+am^2\pi^2]}{8(a^2+4m^2\pi^2)(a^2+m^2\pi^2)};$$

$$h_{110} = \frac{-\pi^4nm^3(-1+e^{4a})}{16a(a^2+m^2\pi^2)};$$

$$A_{10} = \left[\frac{a\pi m(-1+e^{3a}(-1)^m)}{n(9a^2+m^2\pi^2)} + \frac{m\pi(-1+e^{3a}(-1)^m)(-t_2m\pi a+3t_1a^2-n^2t_1a^2+\nu m^2\pi^2t_1+5\nu t_2m\pi a-6\nu t_1a^2)}{an(9a^2+m^2\pi^2)} + \frac{3(-1+e^{3a}(-1)^m)(m\pi t_1a+3t_2a^2-n^2t_2a^2-5\nu m\pi t_1a+\nu t_2m^2\pi^2-6\nu t_2a^2)}{n(9a^2+m^2\pi^2)}\right]$$

$$h_{11} = \frac{m^3\pi^4(e^{4a}-1)[4a^2\pi m(3n^2-1)+(2n^2-1)(m^3\pi^3-2a^3)]}{512a^4(n^2-1)(4a^2+m^2\pi^2)} + \frac{\pi^4m(e^{4a}-1)(a^3-\pi m^3)}{256a^2(n^2-1)(a^2+m^2\pi^2)};$$

$$h_{12} = \frac{-\pi^2m(e^{4a}-1)(2\pi m-a)}{32(a^2+m^2\pi^2)} + \frac{\pi^5m^4(e^{4a}-1)(\pi^2m^2-2a^2)}{32a^2(4a^4+5a^2m^2\pi^2+m^4\pi^4)};$$

$$h_{111} = \frac{n\pi^3m^2(-1+e^{4a})}{16(a^2+m^2\pi^2)};$$

$$h_{21} = \frac{8am^2\pi^2(a-m\pi)(-1+(-1)^me^{3a})}{9n(9a^4+10a^2m^2\pi^2+m^4\pi^4)},$$

$$h_{22} = \frac{4am\pi(-1+(-1)^me^{3a})(-2am\pi+m^2\pi^2+3a^2)}{9n(9a^4+10a^2m^2\pi^2+m^4\pi^4)},$$

$$h_{23} = \frac{160a^2m^2\pi^2(-1+(-1)^me^{5a})}{3n(625a^4+250a^2m^2\pi^2+9m^4\pi^4)},$$

$$h_{24}=\frac{-8a\pi m(-1+(-1)^m e^{5a})(25a^2-3m^2\pi^2)}{3n(625a^4+250a^2m^2\pi^2+9m^4\pi^4)},$$

$$h_{25}=\frac{160a^2m^2\pi^2}{3n(625a^4+250a^2m^2\pi^2+9m^4\pi^4)},$$

$$h_{26}=-h_{24},$$

$$h_{27}=\frac{am\pi^3(-1+(-1)^m e^{5a})}{12n(25a^2+m^2\pi^2)},$$

$$h_{28}=\frac{-40\pi^3m^3a(-1+(-1)^m e^{5a})}{3(625a^4+250a^2m^2\pi^2+9m^4\pi^4)},$$

$$h_{29}=\frac{4m^2\pi^2(-1+(-1)^m e^{5a})(3m^2\pi^2+25a^2)}{3(625a^4+250a^2m^2\pi^2+9m^4\pi^4)},$$

$$h_{210}=\frac{-8m^2\pi^2(-1+(-1)^m e^{5a})(-5a^3+10a^2m\pi+3m^3\pi^3)}{3an(625a^4+250a^2m^2\pi^2+9m^4\pi^4)},$$

$$h_{211}=\frac{4\pi m(-1+(-1)^m e^{5a})(50a^2m\pi-25a^3-3am^2\pi^2+16m^3\pi^3)}{3n(625a^4+250a^2m^2\pi^2+9m^4\pi^4)},$$

$$t_1=\frac{\left\{A\left(1-\beta_1^2-n^2\right)+2B\beta_1\right\}}{\left(A^2+B^2\right)},$$

$$t_2=\frac{\left\{B\left(1-\beta_1^2-n^2\right)+2A\beta_1\right\}}{\left(A^2+B^2\right)},$$

$$t_3=\frac{\left\{C_1\left(-\beta_1n^2+\beta_1-\beta_1^3\right)-64\left(\beta_1^3+\beta_1n^2\right)\beta_1^2\right\}}{4\left[C_1C_2+\left(32\beta_1^3+32\beta_1n^2\right)^2\right]},$$

$$t_4=\frac{\left\{C_2\beta_1^2+16\left(\beta_1^3+\beta_1n^2\right)\left(-\beta_1n^2+\beta_1-\beta_1^3\right)\right\}}{2\left[C_1C_2+\left(32\beta_1^3+32\beta_1n^2\right)^2\right]},$$

$$t_5=\frac{4\left\{(\beta_1^4-\beta_1^2)(\beta_1n^2-\beta_1+\beta_1^3)-4\beta_1^3(\beta_1^2n^2-\beta_1^2)\right\}}{\left(16\beta_1^4-16\beta_1^2\right)^2+1024\beta_1^6},$$

$$t_6=\frac{8\left\{\left(\beta_1^4-\beta_1^2\right)\left(\beta_1^2n^2-\beta_1^2\right)+\left(\beta_1n^2-\beta_1+\beta_1^3\right)\beta_1^3\right\}}{\left(16\beta_1^4-16\beta_1^2\right)^2+1024\beta_1^6},$$

$$\psi=\ln\frac{(2+R_h)}{(2-R_h)};\ \eta=\ln\frac{K_c}{K_m};\ J=K_c+K_m-2K_{cm};\ \frac{R}{h}$$

$$\delta=(\alpha_c+\alpha_m)(E_c+E_m);\ \upsilon=E_{cm}(\alpha_c+\alpha_m)+\alpha_{cm}(E_c+E_m).$$

$$L=\frac{K_{cm}\delta}{J^2}\left[\psi\left(\frac{R}{h}+\frac{1}{2}\right)-1\right]-\frac{\delta}{2J}\left(\psi-\frac{2h}{2R-h}\right)+\frac{\delta}{J^2}(K_m-K_c+\eta K_c)+$$
$$-\frac{K_{cm}\upsilon}{J^2}\left[\frac{R}{h}-\left(\left(\frac{R}{h}\right)^2-\frac{1}{4}\right)\psi\right]-\frac{\upsilon}{J}\left(1-\frac{\psi}{R_h}\right)$$
$$-\frac{\upsilon}{2J^2K_{cm}}\left(K_m^2-K_c^2+2\eta K_mK_c\right)$$
$$+\frac{K_{cm}E_{cm}\alpha_{cm}}{J^2}\left[\frac{1}{9}+\frac{4R^2}{3h^2}-\left(\frac{1}{6}+\frac{4R^3}{3h^3}\right)\psi\right]$$
$$+\frac{2E_{cm}\alpha_{cm}}{J}\left[\frac{h}{6(2R-h)}+\frac{R}{h}-\psi\left(\frac{R}{h}\right)^2\right]$$
$$+\frac{E_{cm}\alpha_{cm}}{9J^2K_{cm}^2}\left[4\left(K_m^3-K_c^3\right)+3K_c\left(K_c^2+3K_m^2\right)\eta\right];$$

$$I=\frac{4K_{cm}}{J^2}\ln\frac{K_c(2R-h)}{K_m(2R+h)}+\frac{8h^2}{J(4R^2-h^2)}.$$

References

Agamirov, V.I., 1990. Dynamic Problems of Nonlinear Shells Theory, science ed. Moscow (in Russian).

Alwar, R.S., Narasimhan, M.C., 1992. The axisymmetric non-linear analysis of laminated orthotropic annular spherical shells. Int. J. Nonlinear Mech. 27 (4), 611–622.

Bagri, A., Eslami, M.R., 2008. Generalized coupled thermoelasticity of functionally graded annular disk considering the Lord–Shulman theory. Compos. Struct. 83, 168–179.

Bich, D.H., Tung, H.V., 2011. Non-linear axisymmetric response of functionally graded shallow spherical shells under uniform external pressure including temperature effects. Int. J. Nonlinear Mech. 46, 1195–2004.

Duc, N.D., Anh, V.T.T., Cong, P.H., 2014. Nonlinear axisymmetric response of FGM shallow spherical shells on elastic foundations under uniform external pressure and temperature. J. Eur. J. Mech. A/Solids 45, 80–89.

Dumir, P.C., 1985. Nonlinear axisymmetric response of orthotropic thin spherical caps on elastic foundations. Int. J. Mech. Sci. 27, 751–760.

Dumir, P.C., Dube, G.P., Mallick, A., 2005. Axisymmetric buckling of laminated thick annular spherical cap. Nonlinear Sci. Numer. Simul. 10, 191–204.

Ganapathi, M., 2007. Dynamic stability characteristics of functionally graded materials shallow spherical shells. J. Compos. Struct. 79, 338–343.

Huang, N.C., 1964. Unsymmetrical buckling of thin shallow spherical shells. J. Appl. Mech. Trans. ASME 31, 447–457.

Kiani, Y., Eslami, M.R., 2013. An exact solution for thermal buckling of annular FGM plates on an elastic medium. Compos. Part B: Eng. 45, 101–110.

Muc, A., 1992. Buckling and postbuckling behavior of laminated shallow spherical shells subjected to external pressure. Int. J. Nonlinear Mech. 27 (3), 465–476.

Nath, N., Alwar, R.,S., 1978. Non-linear static and dynamic response of spherical shells. Int. J. Nonlinear Mech. 13, 157–170.

Prakash, T., Sundararajan, N., Ganapathi, M., 2007. On the nonlinear axisymmetric dynamic buckling behavior of clamped functionally graded spherical caps. J. Sound Vibrat. 299, 36–43.

Shahsiah, R., Eslami, M.R., Naj, R., 2006. Thermal instability of functionally graded shallow spherical shell. J. Therm. Stress. 29 (8), 771–790.

Sofiyev, A.H., 2010. The buckling of FGM truncated conical shells subjected to axial compressive load and resting on Winkler-Pasternak foundations. Int.J. Press. Vessels Pip. 87, 753–761.

Tillman, S.C., 1970. On the buckling behavior of shallow spherical caps under a uniform pressure load. Int. J. Solids Struct. 6, 37–52.

Uemura, M., 1971. Axisymmetrical buckling of an initially deformed shallow spherical shell under external pressure. Int. J. Nonlinear Mech. 6, 177–192.

Wu, C.P., Tsai, Y.H., 2004. The asymptotic DQ solutions of functionally graded annular spherical shells. Eur.. J. Mech. A/Solids 23, 283–299.

Xu, C.S., 1991. Buckling and post-buckling of symmetrically laminated moderately thick spherical caps. Int. J. Solids Struct. 28, 1171–1184.